A METHOD TO CALCULATE THE REAL GAS STAGNATION PROPERTIES FOR SUPERCRITICAL CO2 FLOWS

o Xi Nan, The University of Tokyo, 7-3-1 Hongo Tokyo, E-mail: nan@aero.t.u-tokyo.ac.jp
Takehiro Himeno, The University of Tokyo, E-mail: himeno@aero.t.u-tokyo.ac.jp
Toshinori Watanabe, The University of Tokyo, E-mail: watanabe@aero.t.u-tokyo.ac.jp

This paper focus exclusively on the real gas stagnation properties for sCO2 flows, which are the basic yet very important properties in turbomachinery. When the flow is supercritical, the perfect gas isentropic relations will no longer be valid, especially for the flows near critical point. The equations as well as their physical meanings in fluid dynamic need to be reconsidered. However, unlike the perfect gas, it is practically impossible to obtain an explicit expression of the real gas total quantities. In this paper, a quasi-2D iteration method to obtain real gas stagnation pressure and temperature for sCO2 flows is proposed. By solving the equations of stagnation enthalpy and entropy implicitly, the stagnation pressure and temperature can be accurately calculated without any addendum assumptions. This current method is then applied in several typical cases in order to understand how the total quantities distribute under sCO2 flow conditions.

INTRODUCTION

It is well recognized that the stagnation quantities of flows are very important and necessary throughout the whole design, testing and simulating process for sCO_2 cycles, which is newly emerged power technology relying in the compression process performed close to the critical point of the working fluid [1]. The first typical example could be the sCO_2 compressor aerodynamic performance, in which the compression ratio is characterized by the total pressure ratio, and the efficiency is estimated by the total temperature ratio. The second example is the Pitot tube, in which how to calculate the flow velocity from the measured total and static pressures is a challenge in real gases. The third example appears in CFD. Imposing the total temperature and total pressure as the inlet boundary conditions is a common practice in most turbomachinery simulation, yet it becomes non-trivial in real gas simulation as opposed to ideal gas cases because the static pressure and temperature cannot be found explicitly. The post-processing of the CFD results is the fourth example, in which the static properties and flow velocities are known in prior, yet the stagnation properties have to be calculated in order to understand the physical meanings of the calculated flow fields.

In this paper, we will present a study on how to solve implicit equations for the stagnation (i.e., total) properties without any assumptions for the afore-mentioned fourth example. There are thus two research questions arise:

1. How to calculate the real gas total properties namely total pressure and total temperature given static properties and velocities?
2. Do the total pressure and total temperature represent the same physical meaning as their ideal gas counter parts do?

With the purpose of answering these two questions, studies are conducted as following:

1) Establish a method to calculate the real gas total pressure and total temperature.
2) Investigate the total pressure and total temperature characteristic in typical sCO2 flow cases.

However, it is practically impossible to derive an explicit relation between static to total quantities like their ideal counterparts due to the following reasons. Firstly, modelling the real gas thermal properties such as density or specific heat ratio is a hard task [2, 3]. The current available real gas equations of state or look-up table method [4, 5] appear in extremely complex and nonlinear form. Furthermore, deriving the isentropic relations is another difficult task because we need to deal with the derivatives of the basic thermal properties.

Baltadjiev [6] from MIT established theoretical formulas for real gas isentropic relations. By assuming that the isentropic exponents remain constant from the static to total conditions, the stagnation pressure and temperature can be expressed with a similar form of those for perfect gas. Nederstigt [7] further derived the expressions of total quantities with Peng-Robinson gas with this method. This method involved the fundamental thermaldynamics knowledges, and it is proved to be a fairly good estimation when there is no appreciable difference between the static and total conditions such as low-speed flows. It is also reported that when the sCO2 flow approaches the critical point, the accuracy of this method will diminish. Hence, it still requires a method to be applicable for more general circumstance such as high speed flows or near critical point flows which commonly exist in sCO2 compressors.

In this paper, a method based on a quasi-2D iterations with thermal properties is proposed. This method dependents purely on the thermal properties without introducing any assumption. By definition, the total enthalpy and total entropy must remain constant during the stagnation process. This principle is taken as the key to solve for the pair of total pressure and temperature corresponds to the known static values. It should be pointed out that this method is not restricted to any assumptions on working fluid, flow condition or equation of state. Provided that the static state point and flow velocity are known, its corresponding stagnation point properties can be accurately solved. To model the real gas, the Peng-Robinson equation of state (PR EoS) is adopted in this study. Although this cubic equation model may have some discrepancy near the critical point region, it still shows

good agreement with experimental data in majority of range while keeps the method simple [8, 9].

This paper is organized as following: Firstly, the methodology developed to obtain the real gas total properties are explained in details. Then, two real applications: a Laval Nozzle and a compressor cascade are numerically simulated to investigate the total pressure and total temperature performances in typical sCO2 flows. The total pressure and total temperature under different flow conditions: 1) with and shockwave; 2) trans-critical flow; 3) viscous flow are investigated.

METHDOLOGY

Numerical scheme and real gas model

In this paper, an in-house code named as SHUS was conducted to perform the numerical studies, which was designed to solve the compressible three dimensional Reynolds-averaged Navier–Stokes equations. It was discretized in the computational domain by a cell-centered finite volume formulation. Time integration was accomplished by the Euler implicit method with the lower-upper symmetric Gauss-Seidel scheme (LU-SGS), and no inner iterations were introduced. The inviscid fluxes were evaluated by a simple high-resolution upwind scheme (SHUS), which was extended to third-order accuracy by the MUSCL interpolation via implementing a modified form of Venkatakrishnan's slope limiter. In this code, the solving variations were U, V, W, T and P [10].

To model the real gas, PR EoS is employed. This model was found to be a good compromise between and flexibility while keeping the method simple and relatively of low computational cost according to our previous study of a sCO_2 compressor [8, 9]. The details of this EoS can be found in appendix. Its application and development over 40 years are provided in a comprehensive review literature [11].

For the turbulence calculation respect to sCO_2 flow, the viscous stress tensor was evaluated at the surface of the numerical cell in the central differential manner. The standard two-equation k-ω turbulence model was adopted to evaluate the eddy viscosity, while the viscosity and heat conductivity for the sCO2 fluid are modelled by Chung's method [12] and Scalabrin's model [13] respectively. The flow was treated as fully turbulent without considering any transition of the boundary layer. All the details regarding to the CFD scheme can be found in [14].

Core idea of this method

Figure 1 briefly illustrates the relation between a static local point which is represented by (P, T) and its corresponding stagnation point (P_t, T_t) with temperature- entropy coordinate. According to the definition, the stagnation property is the thermal quantities that flow isentropically decelerates into zero velocity. During this process, the flow experiences adiabatic and reversible stagnation process, yielding:

$$h_t = h + \frac{1}{2}u^2 \quad (1)$$

$$s_t = s \quad (2)$$

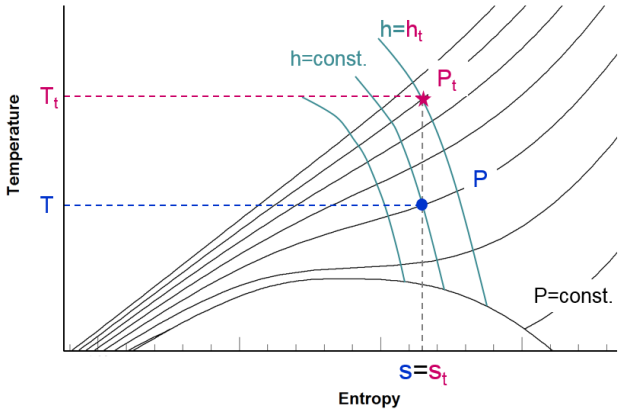

Fig 1 A T-s sketch to illustrate the relation between total quantities and static quantities

Here, the static values of h and s are calculated from the static T and P. Therefore, the task turns to be finding the point (P_t, T_t) satisfying both the entropy value and the total enthalpy value as shown in eq. (1) and (2). To avoid the ambiguity in this section, all the final solutions are called true value in short. Those intermediate variables during the iterations are labelled with superscripts as shown in figure 2.

An implicit method is designed to achieve the (P_t, T_t), which is depended solely on numerical iterations. It is a semi two dimensional iteration procedure as figure 2 shows. Referring to figure 1, the inner iteration is applied along constant entropy curve, aiming at obtaining a bunch of points that yield the true entropy value. The outer iteration is applied to pick up the correct one among these candidates which yields the correct value of total enthalpy. The detailed iteration process are explained as following.

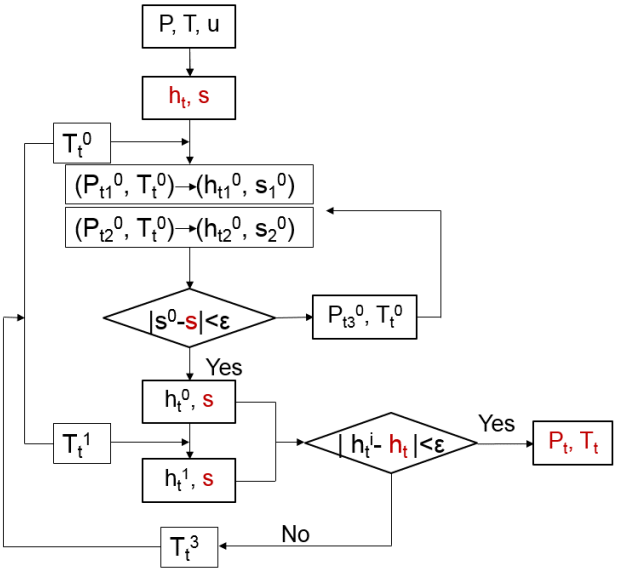

Fig 2 Flowchart of this mythology

STEP 1: obtain Pt0 corresponds to Tt0 maintaining true s

To find the total pressure value corresponds to a fixed total temperate while maintaining the required entropy, it is solved by a one dimensional iteration. The iteration starts with setting an

arbitrary initial total temperature value, labelled as T_{t0} in this paper. Here, the superscript records the iterations. By assuming to arbitrary total pressure values P_{t10} and P_{t20}, the Secant root-finding method can be applied and the solution that yields true value of entropy can be quickly pursued. Figure 3 illustrates this step.

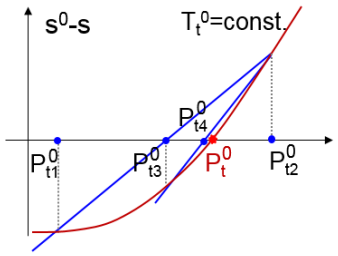

Fig 3 Secant method to solve total pressure that maintain the correct entropy value (take the initial guess T_{t0} of for an example)

Despite the solved P_{t0} yields the true value of entropy, it is certainly not be the expected one corresponding to the true total enthalpy h_t because the total temperature T_{t0} is arbitrarily chosen. Thus, the outer iteration to achieve true total enthalpy by adjusting Tt is required.

STEP 2: iterate the Tt to achieve the true ht

Set another total temperature T_{t1} and repeat step 1, it is consequently obtained the resultant total pressure P_{t1}. The Secant method to achieve true h_t can be initialized by the same way. With several iterations, the pair of (P_t, T_t) that correspond to (P, T) are finally obtained. It should be noticed that each iteration of step 2 contains an execution of step 1, aiming at obtaining the exact P_t that corresponds to each new T_t.

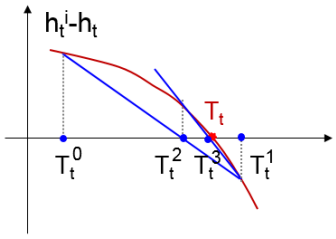

Fig 4 Secant method to peruse the total enthalpy by adjusting the total temperature

This current method avoids to calculate the Mach number and isentropic relations with this current method, only several basic thermal properties are needed. It can be easily extended with real applications as mentioned in introduction by embedded with CFD codes, test data post-processing or turbomachinery analysis.

APPLICATIONS IN CFD STUDIES

The aim of this section is to test this current scheme and investigate the real gas effect on the total pressure and total temperature distributions. Two cases, including inviscid and viscous sCO2 flows are studied.

2-D Laval Nozzle

The study is initialled with a 2-D benchmark Laval nozzle, which is concerned in many research to test numerical scheme in terms of real gas thermal properties prediction [15, 16] or capability of dealing with a wide range of flow conditions. The whole length of the nozzle x_{max}=10cm with the area of throat A_{th}=1cm^2. The position of the throat is exactly the half of the nozzle, ie. x_{th}=5cm. The dimensions of this nozzle is defined as following equations:

$$A(x) = 2.5 + 3\left(\frac{x}{x_{th}} - 1.5\right)\left(\frac{x}{x_{th}}\right)^2 \quad \text{for } x < x_{th} \quad (3)$$

$$A(x) = 3.5 - \frac{x}{x_{th}}\left[6 - 4.5\frac{x}{x_{th}} + \left(\frac{x}{x_{th}}\right)^2\right] \quad \text{for } x \geq x_{th} \quad (4)$$

This nozzle was calculated with 2-D Euler equations. The mesh of studied nozzle was generated with one entire domain with 367863 grid points in total, including 61 points in vertical direction, 201 points in stream direction and 3 points in the third dimension. The inlet boundary was imposed with total pressure and total temperature. Inner iterations are employed to obtain the static pressure and temperature on the first grid centre implicitly. Details of this treatment was published previously in [17]. The slip wall model is applied at solid boundary. Two typical cases: 1) with shockwave and 2) trans-critical flow condition are studied. They are named as CASE A and B respectively. To demonstrate these two cases, figure 5 shows the flow parameter of the nozzle centre line in a P-T coordinate. Especially, the green triangles label the inlet conditions of the two cases.

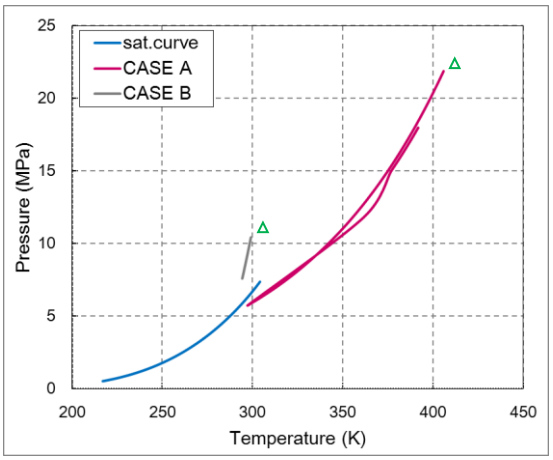

Fig 5 Two study cases in P-T diagram

CASE A: shockwave existing condition

The Case A has a supercritical inflow with total pressure 23.0MPa and total temperature 410K. This inlet condition is far from the critical point. Providing back pressure as 0.83049 times of the inlet static pressure, a normal shock can be generated at about x=7, making the flow approaching to the critical point.

To validate the numerical method, density distribution on the central line are compared with a public result done by Arina [15]. Several van der Walls type EoS were examined in Arina's work and he suggested those theoretical models are quite acceptable. Here, we selected the results predicted by Carbahan-Starling-De Santis (CSD) equation. Meanwhile, to further validate the numerical scheme, calculation was also performed with a commercial software NUMECA with same meshing and computational settings. It is suggested that thermal properties are

solved by look-up table method with the commercial software.

Figure 6 compares the density distributions along the nozzle centre line. Flow accelerates within the converge region at first, and continually this motion passing the throat, reaching the maximum Mach number of 1.6 at the upstream of the shock. It is clearly seen that the shockwave intense and position agree well with each other. A second verification is the Mach number distribution, which is plotted in figure 7.

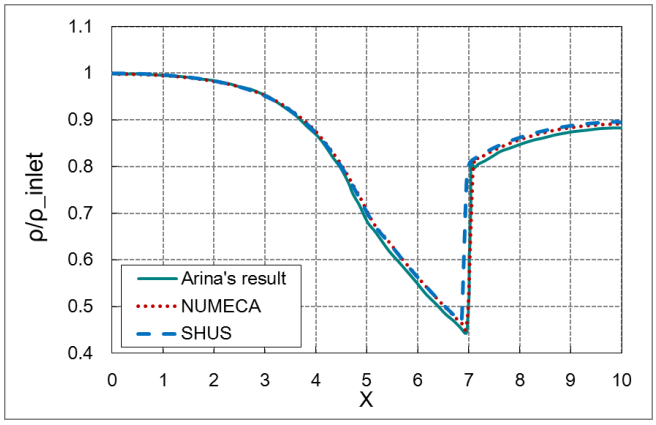

Fig 6 The normalized density distribution along nozzle centre line for Case A

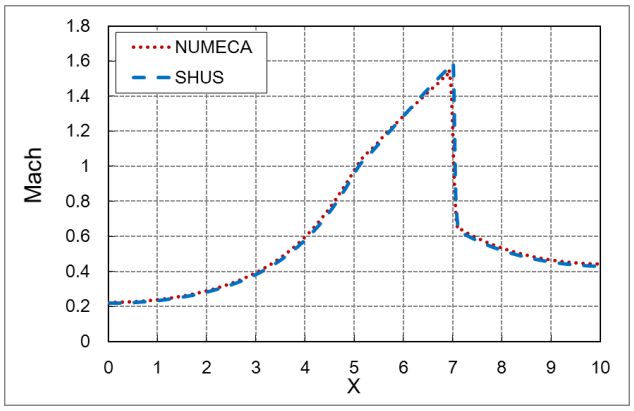

(b) Mach number

Fig 7 Properties distribute along the nozzle central line for Case A

The total pressure and temperature distribution along the nozzle central line is then investigated. Here, the model proposed by Baltadjiev [6] is also involved. For a better understanding, we here take a briefly review for this theoretical model.

Similar to the ideal gas isentropic law pv^{γ}=const, the isentropic process for real gases is established:

$$pv^{n_s} = const \tag{5}$$

$$Tp^{-ms} = const \tag{6}$$

Here n_s and m_s are the isentropic exponents, which are defined as eq. (7-8). There are several ways to treat the thermal property derivative used in these two equations. In this paper, still PR EoS is adopted, taking the advantage its polynomial equation form. Rather than a constant heat ratio γ for the ideal gas, those above isentropic exponents are determined by both temperature and pressure. To adjust a similar equation as ideal gas counterparts, assumption is introduced that these two components maintain constant from static to stagnation conditions. With is simplification, an explicit expression can be derived as shown eq. (9) and (10).

$$n_s = -\frac{v}{P}\frac{c_p}{c_v}\left(\frac{\partial P}{\partial v}\right)_T \tag{7}$$

$$m_s = -\frac{v}{p}\left(\frac{\partial p}{\partial v}\right)_s \tag{8}$$

$$\frac{P_t}{P} = \left[1+\frac{n_s-1}{2}M^2\right]^{\frac{n_s}{n_s-1}} \tag{9}$$

$$\frac{T_t}{T} = \left[1+\frac{n_s-1}{2}M^2\right]^{\frac{m_s n_s}{n_s-1}} \tag{10}$$

The total pressure and total temperature distribution calculated with three different methods are compared in figure 8 and 9 in sequence. It is supposed that the total quantities are constant at the two sides of the shockwave for this inviscid flow, while jump occurs during cross the shock. All methods reproduced this tendency. Oscillation appears in the vicinity of the shock for the commercial software. This oscillation turns to prominent close the shockwave upstream. However, due to lack of information on how to deal with the real gas total properties in this commercial code, the reason is still unclear. Theoretical equation predicts well in majority of the computational domain, however, over-estimation occurs at the upstream of the shock. This discrepancy is amplified as the Mach number exceeds 0.6, see figure 6. Especially when flow approaches to shock, resulting a maximum relative error 6.5% in total pressure and 7.3% in total temperature. It is proved that this theoretical method proposed by MIT researcher can provide a good estimation as long as the Mach number is lower than 0.6.

The real gas effect influence the total properties, which is evidenced by the total temperature distribution. It is recognized that for inviscid flows, total temperature always keeps constant even for flows with shockwave, while, however, this is no longer true for real gases. It is found that the total temperature decreased when the flow cross shock. Same phenomena are also found in [16]. It is considered to be caused by the Joule Thompson effect.

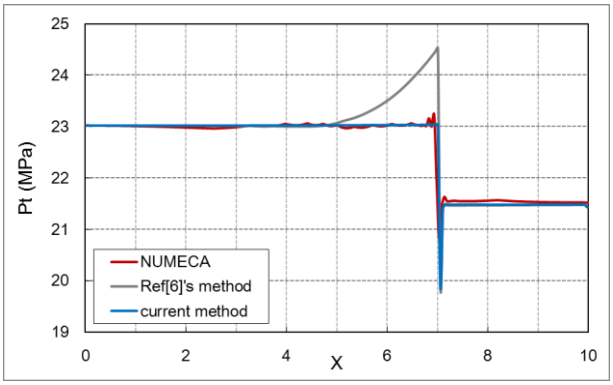

Fig 8 The Pt distribution along the nozzle central line

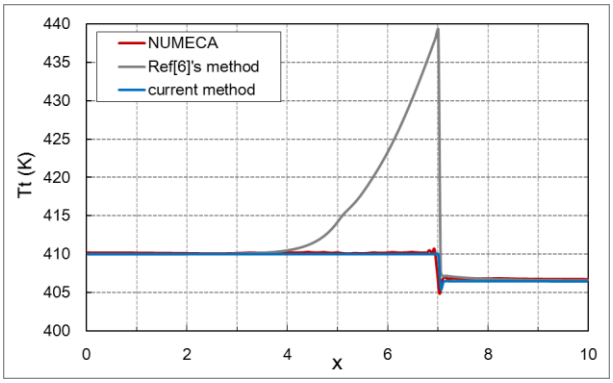

Fig 9 The Tt distribution along the nozzle for Case A

CASE B: trans-critical condition

Another example is concerned under the transcritical flow condition. Inlet total pressure situates at 11Mpa with a total temperature of 300K. In this region, the density is extremely heavy, making the fluid is hard to be compressed. The back pressure was set as 9.5MPa to adjust a low subsonic flow throughout the nozzle.

Figure 10 and 11 present the total pressure and total temperature distribution in following. In respect to total pressure, oscillation appears at the nozzle inlet, outlet as well as throat region. This is considered to be related to numerical unstable yet the whole computation can be achieved converge. Total temperature predicted by this current iteration method almost kept constant, while only less than 0.2% lower-estimated reported by the theoretical method. According to the flow field shown in figure 12, it is regarded to provide same accuracy of these two methods when the flow is low speed.

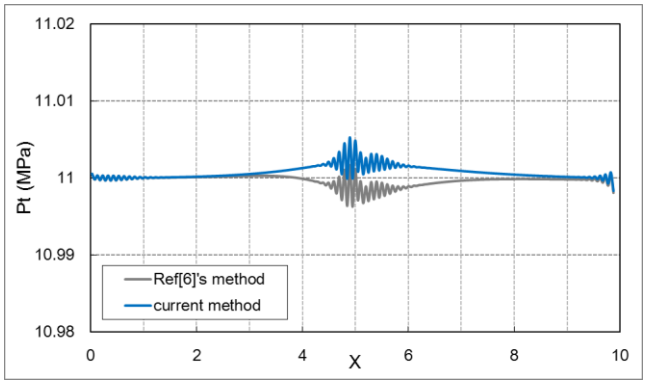

Fig 10 The Pt distribution along the nozzle central line

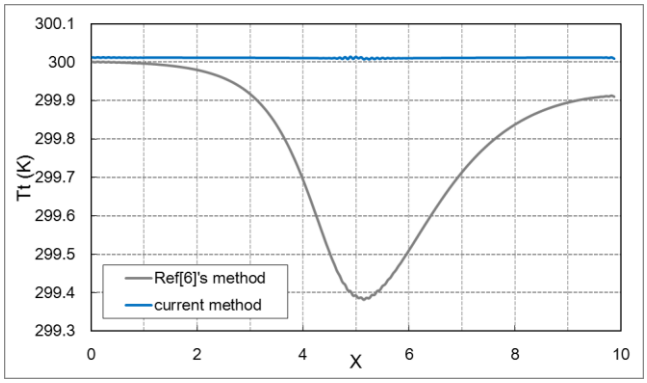

Fig 11 The Tt distribution along the nozzle central line

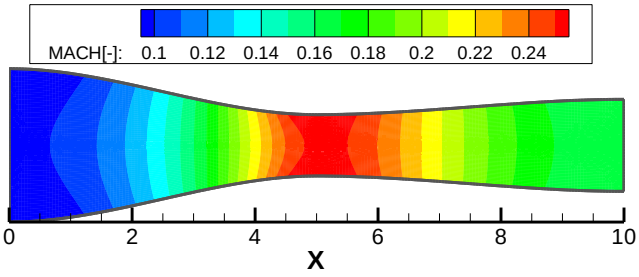

Fig 12 The Mach number distribution along the nozzle central line

2-D compressor cascade

The total pressure characteristic for cascade is used to estimate the blade design or for retrofit purposes. In this section, total pressure loss versus incidence angle with sCO_2 flows are investigated. The compressor cascade C4 was selected, which is a series airfoils containing three different geometries. The profile established with stagger angle of 38° and circular-arc centre line of camber angle 20° was selected. The blade chord was 6 inch, with unity pitch/chord ratio. Despite that this low-speed airfoil is designed with air flow yet may not satisfying the design concept of sCO_2 compressors, we still start with this cascade to gain some basic understanding of the real gas effect on blade performance.

Total pressure, total temperature and flow direction are applied at the inlet boundary while static pressure is fixed at outlet boundary. The inflow Reynolds number was 4,700,000, which was considered as a fully turbulent flow. Experimental data was available only for the air flows, which was done by Rhoden et al. [18]. Due to this reason, the numerical scheme is only validated with air flows. Fixing the inflow velocity of 46m/s, by changing the inflow angle from 35° to 55°, the incidence angle were established with -8°, -4°, +1°, +6°,+11°, respectively.

The total pressure loss is defined as:

$$\varpi = \frac{P_{t1} - \overline{P}_{t2}}{P_{t1} - P_{s1}} \times 100\% \tag{11}$$

Here, the averaged downstream total pressure was measured at one chord downstream of the blade trailing edge. In simulation, identical process method was used. The total pressure was calculated by the current iteration method as forward mentioned.

Figure 13 firstly compares the numerical blade loading coefficient C_p against the tested data. This coefficient is defined as:

$$C_p = \frac{P - P_{s1}}{P_{t1} - P_{s1}} \tag{12}$$

The calculated static pressure distribution agree well with the experimental data, shows the reliability of this current code.

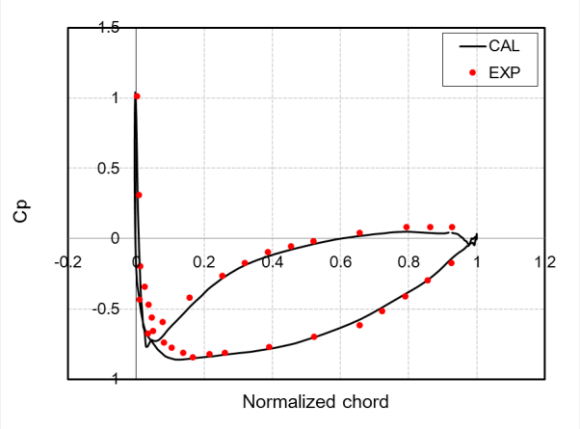

Fig 13 The Cp distribution along blade surface with ideal air at incidence angle of 1°

The performance of total pressure loss with sCO_2 as working fluid is then examined. The characteristic with ideal air, CO_2 under atmosphere and sCO2 conditions are collected in figure 14. For ideal air, the tendency agrees well with test data for the incidence angle while the calculation failed to capture the sharply increased total pressure loss when the incidence angle exceeds +6°. Large discrepancy occurs at large incidence angle. Similar trend displayed when then working fluid was carbon dioxide.

For sCO2 flows, the inlet Mach number equals that for ideal air, 0.135 is set. The total pressure 22Mpa and total temperature 400K were applied at the inlet boundary while back pressure of 21.5MPa was employed. It is shows similar tendency that total pressure loss kept fairly flat in a rather wide inflow angle, while get increased at large negative or positive incidence angles. Furthermore, it is clearly seen that the total pressure loss is almost one third of the normal condition when working fluid is under supercritical condition. The total pressure and total temperature contour are also presented to show the effect of boundary layer and wake in this cascade.

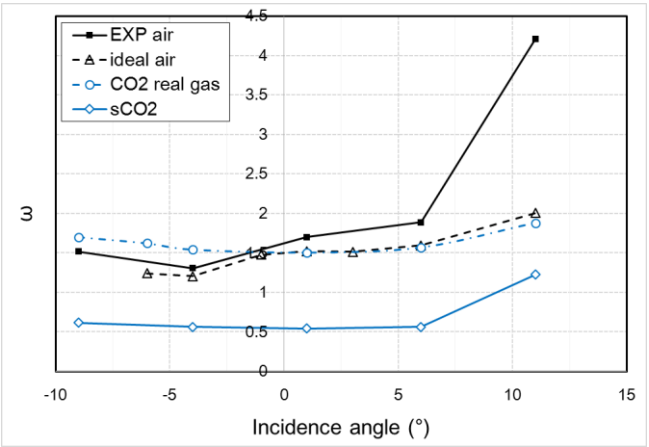

Fig 14 The total pressure loss versus incidence angle at atmosphere and supercritical condition

CONCLUSION REMARKS

A quasi-2D method to calculate total pressure and temperature considering real gas effect is developed in this paper. Due to the difficulties on deriving an explicit expression, an implicit method by purely numerical iterations is designed. This method can be applied for any real gas flows. Total pressure and temperature distributions under several typical supercritical CO_2 flows are analysed by this current method. The flow fields are numerically simulated by an in-house code coupled with Peng-Robinson Equation of State. Conclusions are summarized as following:

1. This current method is established as a quasi-2D iteration. By yielding total enthalpy and entropy as constant values individually, the correct total pressure and total temperature can be implicitly achieved.
2. In each iteration loop, the Secant method is applied to short the root-finding time.
3. It is found that both total pressure and total temperature decrease at the shockwave downstream in a 2-D Laval nozzle, which is the distinct difference with ideal gases.
4. The total pressure and total temperature maintain constant when there is no shockwave for inviscid flows.
5. These above conclusions are also applicable for the sCO2 flows with trans-critical conditions, i.e., liquidous like gases.
6. The performance of total pressure loss against incidence angle for a sCO2 compressor cascade is studied. It is suggested that the total loss coefficient maintains only one third of that for ideal flows with the same inlet Mach number.

This method and findings described above are progress in answering the research question listed in introduction part. They also invite continued refined work and new questions. Further work will carried out with short term and long term categories. In short term, the total pressure loss characteristic under different supercritical flow conditions such as liquid-like region or near critical point need to be carefully investigate. In long term, the real gas flow losses and their mechanisms remain to be quantitatively studied, in order to be applied into sCO2 blade designs.

NOMENCLATURE

Greek letters

U	Velocity in x-direction	m/s
V	Velocity in y-direction	m/s
W	Velocity in z-direction	m/s
T	Static temperate	K
P	Static pressure	Pa
h	Static enthalpy	J kg^{-1} K^{-1}
s	Static entropy	J kg^{-1} K^{-1}
u	Magnitude of flow velocity	m/s
ρ	Density	Kg/m^3

Subscripts

t	Stagnation condition
s	Static condition
1	Inflow measurement station
2	Outflow measurement station

REFERENCES

[1] Raman, S. K., Kim, H. D., (2018), “Solutions of supercritical CO2 flow through a converging-diverging nozzle with real gas effects”. Int. J. Heat Mass Transfer 2018, 116, 127−135.
[2] Rinaldi, E., Pecnik, R., Colonna, P., (2014), “Numerical Computation of the Performance Map of a Supercritical CO2 Radial Compressor by Means of Three-Dimensional CFD Simulations”, ASME paper, GT2014-26966.
[3] Furuzawa, H., Miyazawa, H., Yamanoto, S., (2016), “Numerical Method for Simulating Flows of Supercritical

CO2 Compressor with Nonequilibrium Condensation", ASME paper, GT2016-56431.
[4] Ameli A., Afzalifar A., Turunen-S., Backman J., (2017). "Effects of real gas model accuracy and operating conditions on supercritical CO2 compressor performance and flow field". ASME paper: GT2017-63570.
[5] Fang, Y., Lorenzo , M., Lafon, F., et al., (2018), "An Accurate and Efficient Look-up Table Equation of State for Two-Phase Compressible Flow Simulations of Carbon Dioxide" Ind. Eng. Chem. Res. 2018, 57, 7676−7691.
[6] Baltadjiev, N., (2012), "An investigation of real gas effects in supercritical CO2 compressors", Master's thesis, Massachusetts Institute of Technology, Cambridge, MA.
[7] Nederstigt, P., (2017), "Real Gas Thermodynamics and the isentropic behaviour of substances", Master's thesis, Delft University of Technology.
[8] Tan, T., Himeno, T., Watanabe, T., et al., (2010), "Numerical Analysis of Super-critical Carbon-dioxide Flows in a Centrifugal Compressor", Asian Joint Conference on Propusion and Power, AJCPP2010-157.
[9] Utamura, M., et al., (2012), "Demonstration of Supercritical CO2 Closed Regenerative Brayton Cycle in a Bench Scale Experiment", ASME paper, GT2012-68697.
[10] Sakuma, Y., Watanabe, T., Himeno, T., (2016), "Numerical Analysis of Transonic Compressor with Various Tip Clearance Gap", ASME paper, GT2016-58117.
[11] Lopez-Echeverry, J. S., Reif-Acherman, S., Araujo-Lopez, E. (2017). "Peng-Robinson equation of state: 40 years through cubics. Fluid Phase Equilibria, 447, 39-71.
[12] G.Scalabrin, P.Marchi, and F.Finezzo, (2006), "A Reference Multiparameter Thermal Conductivity Equation for Carbon Dioxide with an Optimized Functional Form", J. Phys. Chem. Ref. Data, Vol.35,No.4, 2006
[13] Bruce E.Poling, John M.Prausnitz, and John P.O'Connell, "The Properties of GASES AND LIQUIDS FIFTH EDITION.
[14] Tan, T., (2009), "Numerical Simulation of a Supercritical Centrigual Compressor", Master Thesis, University of Tokyo.
[15] Arina. R., 2004, "Numerical simulation of near-critical fluids", Applied Numerical Mathematics 51, pp. 409-426.
[16] Jassim E., Abdi M.A., Muzychka Y., (2008), "Computational Fluid Dynamics Study for Flow of Nature Gas through Hihn-pressure Supersonic Nozzles: Part 1: Real gas Effect and shockwave". Petroleum Science and Technology, 26:1757-1772, 2008.
[17] Nan X., Himeno T., Watanabe T., (2018), "The Real Gas Effect on the Inlet Boundary Conditions with Supercritical Carbon Dioxide as Working Fluid", Asia Congress of Gas Turbine, Aguest 22-24, Morioka, Japan, paper 031.
[18] Rhoden H.G., Whsc M.A., (1952), "Effects of Reynolds Number on the Flow of air through a Cascade Compressor Blades", A.R.C Technical Report No. 2919.
[19] Gordon, J., Van Wylen, Borgnakke, C., et al., "Fundamentals of Thermodynamics". Sixth Edition. Property Tables and Charts (SI Units), Appendix 1. ISBN: 9780471428831.

APPENDIX A – Peng-Robinson Equation of State

Since published in 1976, The Peng-Robinson equation of state (PR EoS) has become one of the most useful applied models for thermodynamic and volumetric calculations [11]. It is a van der Waals type of EoS as Eq. (A.1) shows.

$$P = \frac{R_g T}{v-b} - \frac{a}{v(v-b)+b(v-b)} \tag{A.1}$$

The variations quoted in this equation are detailed listed in Table A.1. The real gas density is solved by a cubic equation (A.3), where Z is the compression factor.

$$Z = P/\rho R_g T \tag{A.2}$$

$$Z^3 - (1-B)Z^2 + Z(A-2B-3B^2) - (AB-B^2-B^3) = 0 \tag{A.3}$$

Table A.1 Properties for Peng-Robinson EoS

Symbol	Properties
R_g	Specific gas constant
a	$a = a_c\alpha^2$
b	$b = 0.077796074 R_g T / P_c$
v	Specific volume
Z	Compressible factor
A	$A = aP/(R_g T)^2$
B	$B = bP/R_g T$
α	$\alpha = 1 + f\omega\left(1-\sqrt{T/T_c}\right)$
a_c	$a_c = 0.4572355 R_g{}^2 T_c^2 / P_c$
ω	Acentric factor, ω=0.225
f_ω	$f_\omega = 0.37464 + 1.54226\omega - 0.26992\omega^2$
T_c	Critical temperature, 304.13K
P_c	Critical pressure, 7.3773Mpa
T_r	T_r=T/T_c

APPENDIX B - ENTHALPY AND ENTROPY WITH PR EOS

The real gas enthalpy and entropy are regarded as composed by the departure from ideal gas and the ideal gas value:

$$H = (H - H^{ig}) + (H^{ig} - H_R^{ig}) + H_R^{ig} \tag{B.1}$$

$$S = (S - S^{ig}) + (S^{ig} - S_R^{ig}) + S_R^{ig} \tag{B.2}$$

Where, the superscript "ig" represents ideal gas, while subscript "R" refers to reference state. In this study, reference state was set at 101325pa and 288.15K. The first two terms of the right hand side (H-H^{ig}) and (S-S^{ig}) are the enthalpy and entropy departure functions. For PR EoS, the above equation can be written as:

$$(H - H^{ig}) = R_g T\left(Z - 1 - \frac{A}{2\sqrt{2}B}\left(1 + f_\omega\sqrt{T_r/\alpha}\right)\ln\left(\frac{Z+\left(\sqrt{2}+1\right)B}{Z-\left(\sqrt{2}-1\right)B}\right)\right) \tag{B.3}$$

$$(S - S^{ig}) = R_g \ln(Z-B) - \frac{AR}{2\sqrt{2}B} f_\omega\sqrt{T_r/\alpha}\ln\left(\frac{Z+\left(\sqrt{2}+1\right)B}{Z-\left(\sqrt{2}-1\right)B}\right) \tag{B.4}$$

The second term of the right hind side for eq. (B.1) and (B.2) are temperature depended, which are defined as:

$$(H^{ig} - H_R^{ig}) = C_{pA}(T - T_R) + \frac{1}{2}C_{pB}(T^2 - T_R{}^2) + \frac{1}{3}C_{pC}(T^3 - T_R{}^3) + \frac{1}{4}C_{pD}(T^4 - T_R{}^4) \tag{B.5}$$

$$(S^{ig} - S_R^{ig}) = C_{pA}\ln(T/T_R) + C_{pB}(T - T_R) + \frac{1}{2}C_{pC}(T^2 - T_R{}^2) + \frac{1}{3}C_{pD}(T^3 - T_R{}^3) - R\ln(P/P_R) \tag{B.6}$$

The heat capacity coefficients are the inherent characteristic of CO2, we collected the data in table B.1. The unit for these coefficients are J/(kg K).

Table B.1 C_p coefficients for CO2 [19]

C_{pA}	449.7882958
C_{pB}	1.66863086
C_{pC}	-0.001272878
C_{pD}	3.89759e-07